

Morphometric Study of the Internal Globus Pallidus Using the Robert, Barnard, and Brown Staining Method

Emanuel Cassou dos Santos¹, Djanira Aparecida da Luz Veronez², Daniel Benzecry de Almeida³, Guilherme Santos Piedade¹, Carolina Oldoni¹, Murilo Sousa de Meneses¹⁻³, Mayara Silva Marques³

■ **BACKGROUND:** The globus pallidus internus (Gpi) is a major target in functional neurosurgery. Anatomical studies are crucial for correct planning and good surgical outcomes in this region. The present study described the anatomical coordinates of the Gpi and its relationship with other brain structures and compared the findings with those from previous anatomical studies.

■ **METHODS:** We obtained 35 coronal and 5 horizontal brain specimens from the Department of Anatomy and stained them using the Robert, Barnard, and Brown technique. After excluding defective samples, 60 nuclei were analyzed by assessing their distances to the anatomical references and the trajectories to these nuclei.

■ **RESULTS:** The barycenter of the Gpi was identified at the level of the mammillary bodies and 1 cm above the inter-commissural plane. Thereafter, the distances to other structures were found. The mean \pm standard deviation distance was 15.62 ± 2.66 mm to the wall of the third ventricle and 17.02 ± 2.69 mm to its midline, 4.74 ± 1.12 mm to the optic tract, 2.51 ± 0.8 mm and 13.56 ± 2 mm to the internal and external capsule, and 21.3 ± 2.44 mm to the insular cortex. The cortical point of entry should be located 22.03 ± 4.34 mm to 48.74 ± 4.44 mm from the midline.

■ **CONCLUSION:** The Gpi has less variability in distance to closer anatomical references, such as the optic tract and internal capsule. Distant locations showed a more inhomogeneous pattern. Anatomical studies such as ours are important for the development of new therapeutic

approaches and can be used as a basis for new research involving volumetric and specific group analyses.

INTRODUCTION

The internal segment of the globus pallidus (Gpi) is a relevant part of the diencephalon and is related to motor function and processing and regulating neuronal circuits.¹ Similar to other basal ganglia, this nucleus is involved in the pathophysiology of many movement disorders, such as Parkinson's disease (PD), generalized dystonia, and dyskinesia. Procedures in this region have demonstrated favorable results. Thus, it is a major target for neurosurgical interventions, such as deep brain stimulation and pallidotomy.

The first reported successful surgical procedure in the Gpi dates back to the 1950s; most of these surgeries had been performed to treat PD symptoms.² Despite the clinical advances achieved after the introduction of levodopa therapy, which discouraged functional procedures at the basal ganglia,³ a late follow-up evaluation of these patients revealed that no treatment has been able to avoid the progressive neuronal degeneration in the substantia nigra.⁴ Hence, the need (in late-stage PD) for higher doses of levodopa, with the resultant side effects⁵ (e.g., motor fluctuations and levodopa-induced dyskinesia). This scenario enabled a rebirth of surgical interventions to address symptom relief and the possible reduction of the total required drug dose.⁶

The 2 most performed procedures for PD targeting the Gpi have been deep brain stimulation (DBS) and pallidotomy.⁶ Both procedures have shown improvements in motor function status,

Key words

- Deep brain stimulation
- Internal globus pallidus
- Neuroanatomy
- Pallidotomy
- Parkinson's disease
- Stereotactic atlas

Abbreviations and Acronyms

- DBS:** Deep brain stimulation
- Gpi:** Internal globus pallidus
- MRI:** Magnetic resonance imaging
- PD:** Parkinson's disease

From the ¹Federal University of Parana's Medical School; ²Department of Anatomy, Federal University of Parana, Jardim das Americas; and ³Neurological Institute of Curitiba, Curitiba, Brazil

To whom correspondence should be addressed: Murilo Sousa de Meneses, M.D., Ph.D.
[E-mail: murilomeneses@gmail.com]

Citation: World Neurosurg. (2019).

<https://doi.org/10.1016/j.wneu.2019.02.059>

Journal homepage: www.journals.elsevier.com/world-neurosurgery

Available online: www.sciencedirect.com

1878-8750/\$ - see front matter © 2019 Published by Elsevier Inc.

allowing for some symptom control. However, some studies have shown that the only intervention able to effectively reduce the total levodopa dose (and resulting side effects) was DBS of the subthalamic nucleus.⁶⁻⁸

Neuroanatomical knowledge of the Gpi and its related structures is essential for performing basal ganglia surgery. Two methods are currently in use to target the nucleus and the trajectory to insert the electrode.⁹ In the first method, an indirect location is chosen according to the anatomical landmarks found on imaging examinations (mostly computed tomography or magnetic resonance imaging [MRI]) performed with stereotactic frames. Next, using previous anatomical studies (stereotactic atlases), the distance of the globus pallidus to these structures is measured (i.e., third ventricle, anterior commissure, and posterior commissure). Neurophysiological confirmation with either electrode stimulation or microregistration will usually be needed.¹⁰ In the second method, direct visualization of the globus pallidus is obtained, primarily using MRI studies, to define the borders of the nucleus and the coordinates of the target, with functional confirmation sometimes not required.⁹

Until recently, the indirect method had been used most often.⁶ Technological improvements in MRI acquisition and the use of new sequences have made the direct approach more feasible. Recent advances in neuroimaging techniques have allowed for efficiency in accurately locating the coordinates in the nucleus, with similar postoperative outcomes,^{6,9,11,12} although the coordinates used in these studies differed from the classic stereotactic descriptions of the Gpi.⁹

Anatomical studies of postmortem human brains have set the fundamentals of most stereotactic atlases used in modern neurosurgery.^{13,14} These studies differ widely in their methodological features owing to anatomical research limitations. Furthermore, variations in distinct biotypes have been poorly studied and have likely been underestimated.

We performed an anatomical morphometric study of the Gpi in human brains to analyze the anatomical features of this nucleus, describe its dimensions and distances to other anatomical landmarks, and explore the possible pathways to reach the target in the nucleus.

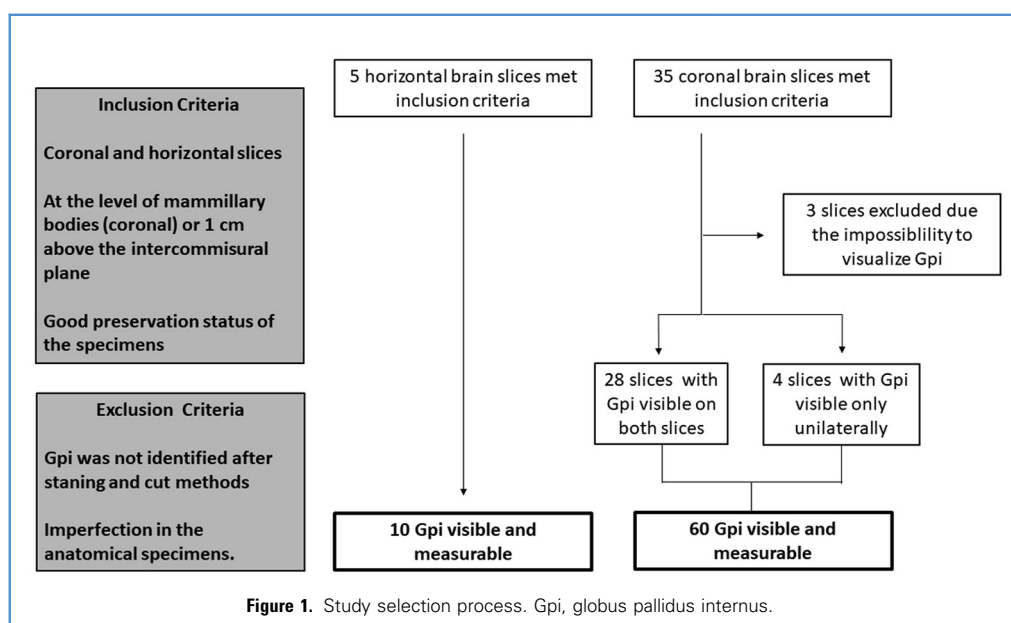
METHODS

Materials and Selection Criteria

A sample of human brain slices with good preservation (obtained from the anatomy department at the Federal University of Parana) was analyzed in the present experimental, descriptive, and analytical study. The ethics committee of the anatomy department at the Federal University of Parana approved the present study. All the brain slices were available for study and research.

The following inclusion criteria were applied: 1) coronal or horizontal slices intersecting the topography of the mammillary bodies and 1 cm above the intercommissural plane; 2) good preservation of the anatomical material that would make the cutting and staining process feasible; and 3) integrity of the globus pallidus after the cutting and staining process. The exclusion criteria were the inability identify the Gpi after the staining and cut process and the presence of any imperfections in the anatomic specimens. The selection process is shown in **Figure 1**.

In the present study, the topography of the coronal slices was established at the level of the anterior portion of the mammillary bodies. This topography was chosen, because it is the anatomically identifiable site closest to the coronal plane that crosses the Gpi targets (i.e., for pallidotomy and DBS), as described previously.¹⁵ Horizontal brain slices were analyzed with the objective of identifying the anatomical landmarks that could locate and confirm the topography used to coronal slice selections.



Material Processing

The slices that fulfilled the inclusion criteria were cut using a stainless steel knife measuring 7-in. long, resulting in slices with a depth of 0.5 cm. This procedure exposed the side of the slice with less of the fixative agent (formaldehyde 10%) and made the staining process possible. All the brain slices were washed for 24 hours in a continuous low-pressure water flow system, avoiding macroscopic damage from the tap water flow¹⁶ and, thereby, preserving the specimens and allowing for removal of the fixative agent.

Staining Technique

The staining technique described by Barnard, Robert, and Brown¹⁷ was used in the present study owing to its greater potential to contrast white and gray matter compared with other techniques.¹⁸ The Barnard, Robert, Brown technique stains the gray matter in blue and leaves the white matter unstained. The method is based on the different physical and chemical properties of the neural tissues. The white matter is lipophilic, capable of binding to phenol and, thus, creating a layer that does not allow further staining by other solutions. The gray matter has a greater iron concentration and can easily react with other substances used with this technique.¹⁹ After staining, all slices were identified to avoid unintended analysis of both sides of the same slice and photographed.

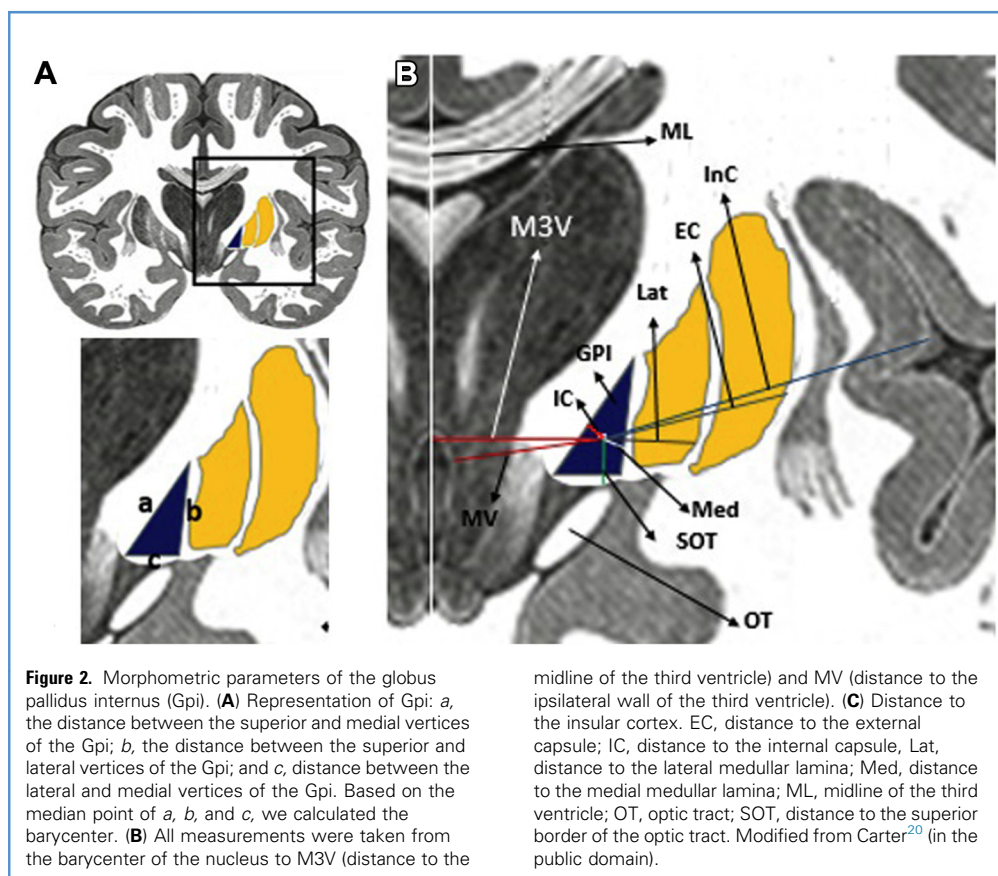
Morphometric Analysis

The Gpi was assumed to be a triangle-shaped structure. Thus, the barycenter (center of mass of a triangle) was defined as the reference to measure the distances from the Gpi to underlying structures (Figure 2) and to further analyze the surgical access trajectories to the nucleus (Figures 3 and 4). Because the present study was mainly of anatomical importance, the barycenter (center of the globus pallidus) was chosen as an important landmark. For neurosurgical reasons, the posteroventral area has usually been chosen for surgical treatment of movement disorders. A more anterior location might be preferred when surgical intervention for psychiatric disorders (e.g., Tourette's disease) is indicated.

The morphometric parameters described were analyzed using public domain software (ImageJ [National Institutes of Health, Bethesda, Maryland, USA]), which allowed for the measurement of distances, angles, and geometric relationships. We also analyzed these measurements using electronic calipers (resolution power, 0.01 mm).

Statistical Analysis

Student's *t* tests were performed to verify the differences between the 2 methods used to access the morphometric parameters of the Gpi. We considered a *P* value of <0.05 to indicate statistical significance.



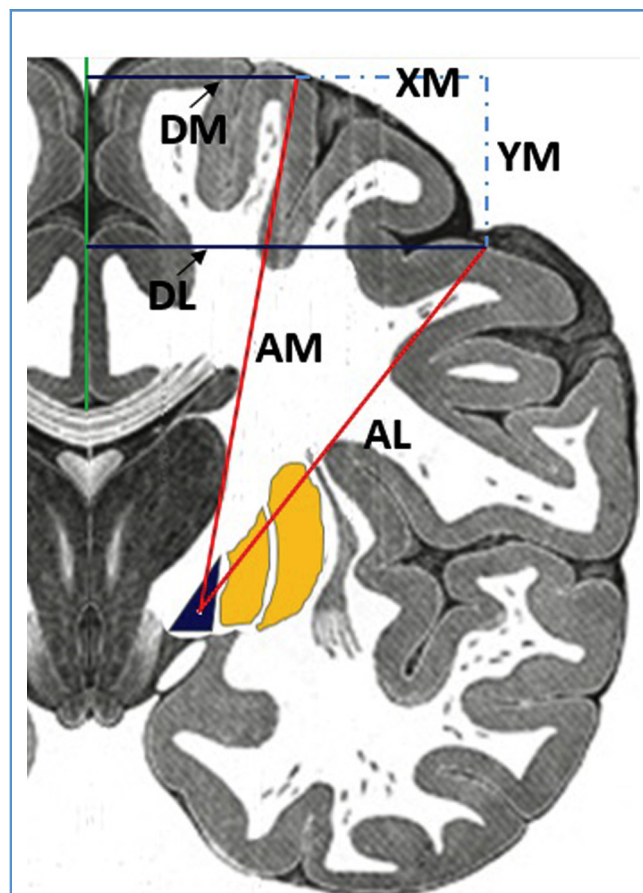


Figure 3. Possible pathways to reach the globus pallidus internus (Gpi) for electrode insertion. From the barycenter of the nucleus, we drew 2 lines at the most medial limit, which crossed the lateral border of the caudate nucleus, and at the most lateral limit, which crossed the insular cortex. Both trajectories have entrance points on the cortical surface of the frontal lobe. The angles described by both trajectories were measured. AM, distance from the barycenter to the medial entrance point; AL, distance from the barycenter to the lateral entrance point; DM, distance from the medial entrance point to the midline; DL, distance from the lateral entrance point to the midline; XM, distance between both entrances points on the horizontal axis; YM, distance between both entrances points on the vertical axis. Modified from Carter²⁰ (in the public domain).

RESULTS

After the staining process, 35 coronal (Figures 5 and 6) and 5 horizontal brain slices (Figure 7) were analyzed, resulting in 60 Gpi that met the selection criteria on the coronal plane and 10 nuclei on the horizontal plane. After staining, it was not possible to identify the nuclei bilaterally in 3 slices, which led to their exclusion from the analysis. In 4 slices, the nucleus was measurable on only 1 side (right or left).

Horizontal Slices

The analysis of the horizontal slices showed that the coronal plane that crossed the intercommissural line 2–3 mm anterior to its midpoint (mid-commissural point) was at the same level of the

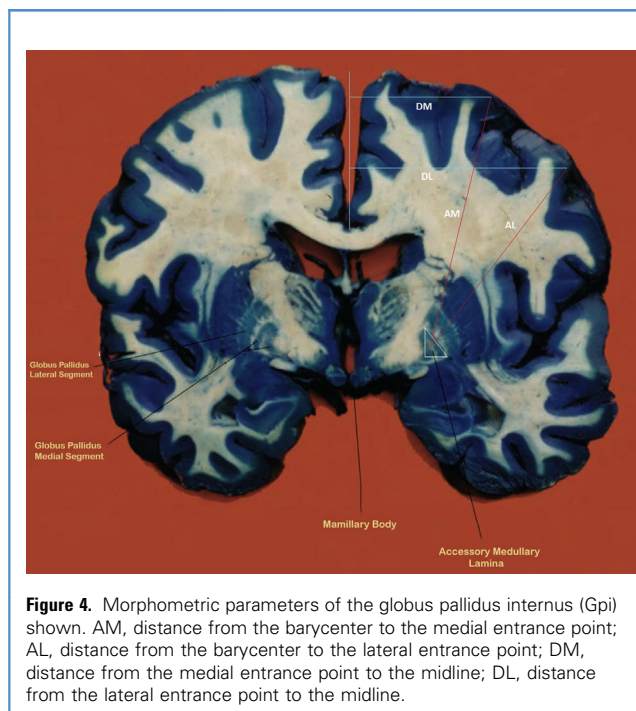


Figure 4. Morphometric parameters of the globus pallidus internus (Gpi) shown. AM, distance from the barycenter to the medial entrance point; AL, distance from the barycenter to the lateral entrance point; DM, distance from the medial entrance point to the midline; DL, distance from the lateral entrance point to the midline.

mammillothalamic fasciculus, the superior efferent projection of the mammillary bodies (Figure 7).

Coronal Slices

Morphometry and Gpi Dimensions. The morphometric analysis showed that the medial side was the largest (8.65 ± 1.25 mm) and the inferior side was the smallest (6.3 ± 1.24 mm) using both methods (software image analysis and mechanical measuring using the calipers; Table 1). The differences in the 3 measurements taken using ImageJ compared with those taken

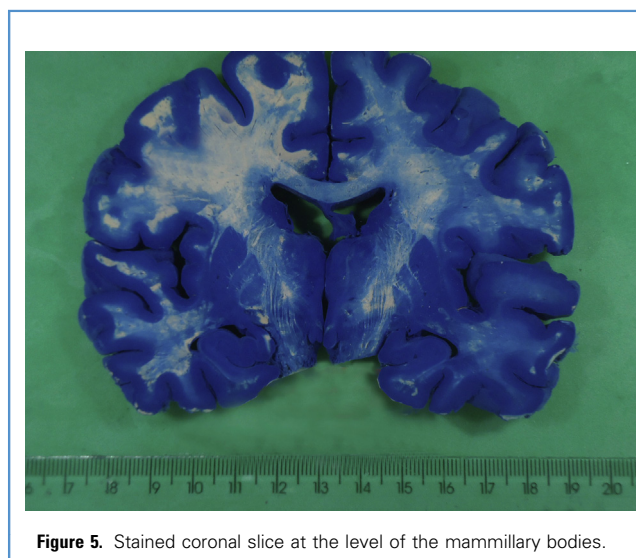


Figure 5. Stained coronal slice at the level of the mammillary bodies.

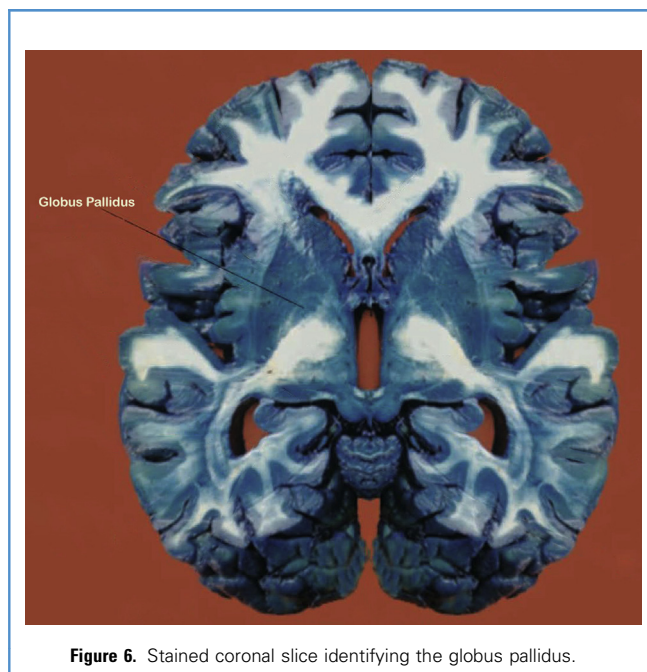


Figure 6. Stained coronal slice identifying the globus pallidus.

using the calipers proved to be statistically significant ($P < 0.05$; [Table 1](#)).

Distance to Anatomical References. Assuming that the barycenter of the Gpi is a geometric standard reference for the morphometric analysis of the nucleus, the Gpi was found to be 15.62 ± 2.66 mm from the ipsilateral wall of the third ventricle and 17.02 ± 2.69 mm

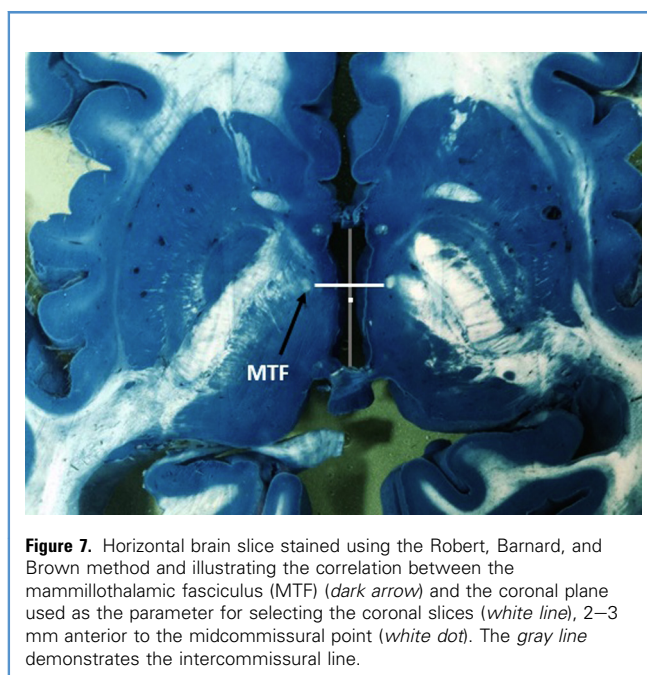


Figure 7. Horizontal brain slice stained using the Robert, Barnard, and Brown method and illustrating the correlation between the mammillothalamic fasciculus (MTF) (dark arrow) and the coronal plane used as the parameter for selecting the coronal slices (white line), 2–3 mm anterior to the midcommissural point (white dot). The gray line demonstrates the intercommissural line.

Table 1. Measurement Results of Sides of Globus Pallidus Internus and Distances From Barycenter of the Nucleus to the Anatomical Landmarks

Variable	Measurements with Calipers (mm)	Measurements with ImageJ (mm)	P Value
Morphometric parameter			
Length of medial side	7.4 ± 0.97	8.65 ± 1.25	<0.0001
Length of lateral side	7.3 ± 0.91	7.98 ± 1.17	0.0041
Length of inferior side	5.56 ± 1.12	6.3 ± 1.24	0.0053
Distance to different structures			
Wall of third ventricle	15.11 ± 2.45	15.62 ± 2.66	0.36
Midline of third ventricle	16.29 ± 2.5	17.02 ± 2.69	0.2
Insular cortex	21.57 ± 2.38	21.63 ± 2.44	0.91
External capsule	13.13 ± 1.81	13.53 ± 2	0.35
Lateral medullary lamina	6.99 ± 1.18	7.44 ± 1.08	0.063
Medial medullary lamina	3.29 ± 0.76	3.58 ± 0.75	0.08
Optic tract	4.25 ± 1.35	4.74 ± 1.12	0.0599
Internal capsule	NA	2.51 ± 0.8	NA
Data presented as mean \pm standard deviation. NA, not applicable.			

from its midline. We also obtained a distance of 21.63 ± 2.44 mm to the insular cortex.

For the measurements taken from the landmarks of the lenti-form nucleus and related structures, the Gpi was found to be at a distance of 13.53 ± 2 mm to the external capsule (lateral border of the putamen), 7.44 ± 1.08 mm to the lateral medullary lamina, and 3.58 ± 0.75 mm from the medial medullary lamina (the group of fibers that separates the Gpi from the external globus pallidus). The distances to the superior border of the optic tract (4.74 ± 1.12 mm) and the internal capsule (2.51 ± 0.8 mm) were also obtained from the analysis. The results are shown in [Table 1](#). The distances measured from these landmarks were not significantly different statistically between the 2 methods.

Access Pathways. The analysis of the access pathways and electrode insertion ([Table 2](#)) showed that the medial pathway, which crosses the lateral border of the caudate nucleus, measured 22.03 ± 4.34 mm from the midline, at an angle of $5.44^\circ \pm 5.29^\circ$ from the mean plane. Its total length (from the entrance on the cortex to the barycenter) was 61.54 ± 5.45 mm.

Table 2. Morphometry of Access Pathways to Globus Pallidus Internus

Variable	Mean \pm SD
Entrance point of the medial access pathway	
Distance to midline (mm)	22.03 \pm 4.34
Angle of trajectory ($^{\circ}$)	5.44 \pm 5.29
Distance to barycenter of Gpi (mm)	61.54 \pm 5.45
Entrance point of lateral access pathway	
Distance to midline (mm)	48.74 \pm 4.44
Angle of trajectory ($^{\circ}$)	35.14 \pm 5.91
Distance to barycenter of Gpi (mm)	55.87 \pm 4.74
Distance between access points of both pathways (mm)	
Horizontal	26.56 \pm 4.9
Vertical	15.54 \pm 4.55

SD, standard deviation; Gpi, globus pallidus internus.

The lateral access, which crosses the border of the insular cortex, was 48.74 ± 4.44 mm from the midline, $35.14^{\circ} \pm 5.91^{\circ}$ from the mean plane, and had a trajectory of 55.87 ± 4.74 mm in length. The results from the measurements taken from the parameters related to the access pathways described in the present study are shown in **Table 2**.

DISCUSSION

The present study has produced a detailed morphometric analysis of the Gpi, describing its relationship to nearby structures and possible surgical approaches. In a sample of 35 coronal slices, we obtained 60 nuclei, which allowed for enough data to consider individual variability in a South American cohort.

Most currently available neuroanatomical stereotactic research in human brain specimens has been related to several atlases developed to guide functional neurosurgical procedures. These have differed widely in both method and anatomical landmarks.¹³

The first stereotactic atlas, reported by Spiegel and Wycsis²¹ in 1952, was based on a series of 30 unstained and myelin-stained coronal, sagittal, and oblique brain slices originating from 1 brain and cut at a regular distance from the posterior commissure. Their atlas established that mark (along with the midline) as the referential marks for diverse anatomical structures.

Talairach et al.²² in 1957, studied unstained and myelin-stained brain slices from 1 brain. The greatest contribution of their work was the establishment of the intercommissural line as a major stereotactic reference. The second version of this atlas in 1988,²³ one of the best known atlases in stereotactic surgery, was based on a study of 36 sagittal slices from 1 brain. Image reconstruction allowed for the creation of 38 coronal and 27 horizontal slices. The atlas proposed a coordinate adjustment system to compensate for individual variations in brain size and also enabled overlapping with radiological images.²³

Schaltenbrand and Bailey²⁴ in 1959 analyzed 111 unstained brain slices in the horizontal, sagittal, and coronal planes. They set the basis for one of the most used stereotactic atlases. In the second version in 1976, Schaltenbrand and Wahren²⁵ performed a detailed histological analysis of the regions most relevant to stereotactic surgery. The data were obtained from a large sample. Seven brains were analyzed to quantify the variability, and 34 of the remaining slices underwent macroscopic study (19 coronal, 5 sagittal, and 6 horizontal). The other slices were studied using microscopic histological techniques.

More recently, atlases have tended to combine radiological MRI analysis with histochemical or immunohistochemical techniques. Morel,²⁶ in 2007, reported a stereotactic study of the basal ganglia and the thalamus using these techniques. In addition, tridimensional atlases using mathematical algorithm models have been created to convert printed atlases into 3 dimensions.²⁷

In the present study, we found less variation in the distances from the anatomical landmarks closer to the Gpi (e.g., the internal capsule, medullary medial lamina, optic tract, and medial medullary lamina). This implies that, in this topography, the relationship of the Gpi to these structures is more constant. Structures distant from the barycenter (e.g., the midline and wall of the third ventricle and insular cortex) showed greater variability in the distance. This could be related to either population heterogeneity^{13,15,23} or to factors related to the internal validity (sample selection) of the study (addressed in subsequent paragraphs).

The differences between the 2 methods we used to evaluate the morphometry of the Gpi (i.e., the dimensions of the Gpi using direct measurement with calipers and software analysis) showed that the first method might be less reliable when estimating the actual lengths of the nuclei. This finding likely resulted from the greater difficulty in determining the boundaries of the nucleus using only the resolution of the naked eye. Software analysis allowed for contrast enhancement and zoom properties that eased the task of discerning the nuclei limits. Only the dimensional analysis showed differences between the 2 methods. The differences in the other measures were not significantly different statistically.

The distances between the barycenter and the midline (17.02 mm) and the ipsilateral wall of the third ventricle (15.62 mm) found in the present study were less than those described in previous studies, specifically the target of pallidotomy (classically, 18–21 mm from the midline)²⁸ and DBS of the Gpi (17.5 mm lateral to the wall of the third ventricle¹⁵). This difference could have been because the barycenter (the reference we used as a geometric standard mark and, thus, generalized to all nuclei) did not align with the targeted coordinates for electrode insertion. This finding might have been because the targets used for pallidotomy and DBS are at the inferior and medial parts of the nucleus, the region responsible for the sensorimotor function of the nucleus.^{3,6,29}

The great variability described in the present study concerning the distance from the midline of the third ventricle (± 2.69) could be explained by sample heterogeneity because the specimens demonstrated greater brain atrophy and were likely from an older population.

Regarding the other anatomical references, the distance from the barycenter to the internal capsule (2.51 mm) was less than the target described for DBS implantation (3–4 mm lateral to the internal capsule¹⁵). This finding is important to establish a safety margin to avoid stimulation of this structure, which could induce contralateral motor problems in the patient. The distance to the medial medullary lamina (3.58 mm) was similar to the measurements described for DBS (4 mm lateral),¹⁵ with the aim of not stimulating the external globus pallidus, which could impair the final result. The electrode insertion area has been described by many investigators as inferior to the barycenter and close to the superior border of the optic tract.¹⁰

Laitinen et al.²⁸ in 1992 described an access pathway performed through a burr hole located 2 cm (20 mm) from the midline and 1.5 mm anterior to the coronal suture to avoid eloquent areas of the brain. Other alternative approaches have been reported, using an access lateral to that classically described, such as an entrance point 2.5–3 cm from the midline.¹⁵ The findings from the present study have shown that the medial access pathway measures 22.03 mm from the midline. The standard technique considers a parasagittal trajectory (0° angle) that is adjustable for lateral or medial corrections, according to the individual anatomy of the patient and to avoid the lateral ventricle or sulcus (given the risk of hemorrhagic events).^{10,15,28} The angle described in the present study for medial access was in accordance with those reported in previous studies (5.44° and a standard deviation of approximately the same magnitude 5.29°).

The lateral access limits (without penetrating the insula) were located 48 mm from the midline, producing a 35.14° angle. A far lateral access could be related to lesions in the branches of the middle cerebral artery and, thus, result in a greater intracranial hemorrhage risk (a complication reported in 2% of the patients^{12,14,16}). Therefore, an approach that lies between the 2 limits described would be preferred, such as performing a trajectory that primarily follows through the internal capsule, reducing the risk of vascular lesions and intracranial hemorrhage. This access could measure 2.2–4.8 cm lateral to the midline. However, the electrode inclination angle (on the y-axis) is critical to ensure success of the elliptical lesions for pallidotomy.¹⁰

More recently, some small studies have compared the electrode insertion using the atlas location, with electrophysiological confirmation provided for indirect MRI-guided targeting of the

Gpi alone.^{9,11,12} Although some reports have suggested that a difference exists in the location between these 2 methods (usually the target calculated by the direct method will be more medial, inferior, and posterior compared with the locations in the atlases⁹), the clinical outcomes have seemed to demonstrate no differences between the 2 groups. In addition, surgeons should not underestimate the contributions of several anatomical studies to stereotactic functional surgery, because most anatomical reference structures and systems, such as the intercommissural plane, were based on analyses of human brains. Furthermore, additional studies with larger sample sizes are still needed to effectively compare the 2 methods.

The present study had some limitations, which primarily resulted from the technical difficulties of anatomical studies. Our sample presented a heterogeneity that was likely related to the following: 1) the age of the specimens; 2) a fixation time >6 weeks¹⁶; 3) the interval between fixation and brain extraction; and 4) the effect of the formaldehyde fixative solution on the brain (a heterogeneous volume increase in some regions of the brain within the first 5 days of fixation with a later volume reduction). However, the effect of formaldehyde in our series might not have been significant because the effect was described for regions of the brainstem and not for the basal ganglia.³⁰

CONCLUSION

The results from the present study have demonstrated that the internal segment of the globus pallidus (on the coronal plane in the topography of mammillary bodies) has a constant anatomic relationship with nearby structures (internal capsule, medial medullary lamina, optic tract) and a more variable relationship with distant marks (midline and wall of the third ventricle).

Anatomical studies such as ours are of major importance in planning strategies for diagnosis and therapeutic interventions. In the future, volumetric studies of the globus pallidus could contribute to a better understanding of degenerative diseases. Moreover, additional studies depicting the neural circuits in the basal ganglia and the anatomical variation according to gender and ethnicity are needed.

ACKNOWLEDGMENTS

We thank the American Journal Experts (AJE) for language editing.

REFERENCES

- Brodal P. The basal ganglia. In: Brodal P, ed. *The Central Nervous System*. 4th ed. New York, NY: Oxford; 2010:324-342.
- Lanska DJ. The history of movement disorders. In: Finger S, Boller F, Tyler KL, eds. *Handbook of Clinical Neurology*. Vol. 95. New York, NY: Elsevier; 2009:501-546.
- DeLong MR, Wichmann T. Basal ganglia circuits as targets for neuromodulation in Parkinson disease. *JAMA Neurol*. 2015;172:1354-1360.
- Olanow CW. Levodopa: effect on cell death and the natural history of Parkinson's disease. *Mov Disord*. 2015;30:37-44.
- Aquino CC, Fox SH. Clinical spectrum of levodopa-induced complications. *Mov Disord*. 2015; 30:80-89.
- Metman LV, Slavin KV. Advances in functional neurosurgery for Parkinson's disease. *Mov Disord*. 2015;30:1461-1470.
- Follett KA, Weaver FM, Stern M, et al. Pallidal versus subthalamic deep-brain stimulation for Parkinson's disease. *N Engl J Med*. 2010;362: 2077-2091.
- Deuschl G, Schade-Brittinger C, Krack P, et al. A randomized trial of deep-brain stimulation for Parkinson's disease. *N Engl J Med*. 2006;355: 896-908.
- Nowacki A, Fiechter M, Fichtner J, et al. Using MDEFT MRI sequences to target the Gpi in DBS surgery. *PLoS One*. 2015;10:1-15.
- Vitek JL, Bakay RA, Hashimoto T, et al. Micro-electrode-guided pallidotomy: technical approach and its application in medically intractable Parkinson's disease. *J Neurosurg*. 1998;88:1027-1043.
- Park SC, Lee CS, Kim SM, Choi EJ, Lee JK. Comparison of the stereotactic accuracies of function-guided deep brain stimulation, calculated using multitrack target locations geometrically inferred from three-dimensional trajectory rotations, and of magnetic resonance imaging-guided deep brain stimulation and outcomes. *World Neurosurg*. 2016;98:734-749.

12. Sidiropoulos C, Rammo R, Merker B, et al. Intraoperative MRI for deep brain stimulation lead placement in Parkinson's disease: 1 year motor and neuropsychological outcomes. *J Neurol*. 2016; 263:1226-1231.
13. Alho E, Grinberg L, Heinsen H, Fonoff ET. Review of printed and electronic atlases of the human brain. In: Peres JFP, ed. *Neuroimaging for Clinicians—Combining Research and Practice*. Rijeka, Croatia: InTech; 2011:145-171.
14. Coffey RJ. Printed stereotactic atlases, review. In: Lozano AM, Gildenberg PL, Tasker RR, eds. *Textbook of Stereotactic and Functional Neurosurgery*. 2nd ed. Berlin, Germany: Springer-Verlag; 2009: 347-372.
15. Starr PA. Placement of deep brain stimulators into the subthalamic nucleus or globus pallidus internus: technical approach. *Stereotact Funct Neurosurg*. 2002;79:118-145.
16. Roberts M. Preparation of brain slices for macroscopic study by the copper sulfate-phenol-ferrocyanide technique. *Stain Technol*. 1969;44: 143-146.
17. Barnard JW, Robert JO, Brown JC. A simple macroscopic staining, and mounting, procedure for wet section from cadaver brains. *Anat Rec*. 1949; 105:1-17.
18. Meneses MS, Montano PJC, Fuzza RF, Buzetti MJ. Análise comparativa de cortes de encéfalos humanos com coloração por três técnicas diferentes. *Arq Neuropsiquiatr*. 2004;62(suppl 2A): 276-281.
19. Kramer FM. Macroscopic staining of the brain. *J Anat*. 1938;72:625-626.
20. Carter HK. Plate 718. In: Gray H, ed. *Anatomy of the Human Body*. 20th ed. Philadelphia, PA: Lea & Febiger; 1918:718.
21. Spiegel EA, Wycis HT. *Stereoccephalotomy (Thalamotomy and Related Procedures)*. New York, NY: Grune and Stratton; 1952.
22. Talairach J, David M, Tournoux P, Kvasina P. *Atlas D'Anatomie Stereotaxique: Réperage Radiologique Indirect Des Noyaux Gris Centraux Des Régions Mesencephalo-Sousoptique et Hypothalamique de L'Homme*. Paris, France: Masson & Cie; 1957.
23. Talairach J, Tournoux P. *Co-planar Stereotaxic Atlas of the Human Brain: Three-Dimensional Proportional System: An Approach to Cerebral Imaging*. New York, NY: Thieme Publishers; 1988.
24. Schaltenbrand G, Bailey P. *Introduction to Stereotaxis with an Atlas of the Human Brain*. Stuttgart, Germany: Thieme Publishers; 1959.
25. Schaltenbrand G, Wahren W. *Atlas for Stereotaxy of the Human Brain with an Accompanying Guide*. Stuttgart, Germany: Thieme Publishers; 1976.
26. Morel A. *Stereotactic Atlas of the Human Thalamus and Basal Ganglia*. New York, NY: Informa Healthcare; 2007.
27. Yelnik J, Bardinet E, Dormont D, et al. A three-dimensional, histological and deformable atlas of the human basal ganglia. I. Atlas construction based on immunohistochemical and MRI data. *Neuroimage*. 2007;34:618-638.
28. Laitinen LV, Bergenheim AT, Hariz MI. Leksell's posteroventral pallidotomy in the treatment of Parkinson's disease. *J Neurosurg*. 1992;76:53-61.
29. Wichmann T, DeLong MR. Deep-brain stimulation for basal ganglia disorders. *Basal Ganglia*. 2011;1:65-77.
30. Quester R, Schröder R. The shrinkage of the human brain stem during formalin fixation and embedding in paraffin. *J Neurosci Methods*. 1997;75: 81-89.

Conflict of interest statement: The authors declare that the article content was composed in the absence of any commercial or financial relationships that could be construed as a potential conflict of interest.

Received 7 June 2017; accepted 14 February 2019

Citation: World Neurosurg. (2019).

<https://doi.org/10.1016/j.wneu.2019.02.059>

Journal homepage: www.journals.elsevier.com/world-neurosurgery

Available online: www.sciencedirect.com

1878-8750/\$ - see front matter © 2019 Published by Elsevier Inc.